Coulomb blockade in ion-induced electron emission and neutralization mechanisms

N. Bajales,[1] J. Ferrón,[1,2] and E. C. Goldberg[1,2]
[1]*Instituto de Desarrollo Tecnológico para la Industria Química, Investigaciones Científicas y Técnicas and Universidad Nacional del Litoral, Güemes 3450 CC 91, 3000 Santa Fe, Argentina*
[2]*Departamento de Materiales, Facultad de Ingeniería Química, Consejo Nacional de Investigaciones Científicas y Técnicas and Universidad Nacional del Litoral, Güemes 3450 CC 91, 3000 Santa Fe, Argentina*
(Received 9 June 2007; revised manuscript received 17 September 2007; published 26 December 2007)

We present a time-dependent quantum mechanical calculation of the charge transfer process in He^+/Al collision, where the resonant neutralization to the ground and first excited states of He is taken into account in a correlated way according to a Coulomb blockade effect. Our results provide an explanation to the discrepancies still found between theory and experiments in low energy ion scattering for this system, as well as allow us to understand the presence of high energy electrons in ion induced secondary electron emission spectra.

DOI: 10.1103/PhysRevB.76.245431 PACS number(s): 73.23.Hk, 68.49.Sf, 79.20.Rf

I. INTRODUCTION

The interaction of low energy ions with solids is a very complex process where several different basic physical mechanisms are involved. It is, on the other hand, the basis of some of the most important surface characterization techniques, being the quality of a specific technique determined by the balance of such mechanisms. For instance, the large elastic cross section and the inelastic processes, ruled by electron transitions, of low-energy-ions–surface collisions are the responsible for the extremely large surface sensitivity of a technique like low energy ions spectrometry (LEIS), and also of its poor quality when speaking about quantification.

As Aluminum (Al) is a prototypical free-electron metal and helium (He) the simplest noble gas, it is natural that the He^+/Al surface collision system has been usually chosen as a model system for ion-surface collisions. Since the helium ionization level falls below the bottom of the Al valence band, no resonant neutralization to this level is expected, turning the Auger process the obvious neutralization mechanism (AN).[1] Thus, ion neutralization, the key process in LEIS, appears to be coupled to secondary electrons emission through the AN mechanism. However, neutralization probability calculations applied to the LEIS regime based only on AN show major discrepancies with experiments. The inclusion of resonant neutralization to the He ground state, operative at close distances due to the He 1*s* level promotion, improves the agreement between theory and experiment, but it is still insufficient to completely accounts for the large observed neutralization of He^+ at the Al surface.[2,3]

It has been stated that resonant neutralization to the first excited level of the noble gas ions is only possible for low work function metals, depending its extent on the ionization potential of the first excited level and the velocity of the ion.[4] There is, however, new experimental evidence showing that ion neutralization at clean, high-work-function metal surfaces occurs at much smaller ion-surface separations than inferred from earlier measurements of ion scattering. Thus, through the strong short-range chemical interactions between incident ion and neighboring metal atom, the energy level shifts should be more important than previously thought.[5,6] Calculations of the helium $n=2$ state levels near an aluminum surface show that, whereas these levels initially move up in energy as the surface is approached, close to the surface, the short-range interactions lead to a lowering of their energies. At smaller atom-surface distances, the levels again rise but their widths should be, at this point, large enough to ensure that they extend below the Fermi energy.[7,8] There has been already an attempt to explain the neutralization behavior of 1–5 keV He^+ ions, scattered from clean metal surfaces, based on the resonant charge transfer from the surface valence band to the He 2*s* level.[9] In that work, it is considered that when a He^+ approaches a surface, it is energetically favorable for the He-surface system to screen the 1*s* core hole by putting an electron in the 2*s* level. However, the resonant charge transfer to the He 2*s* level was calculated finally by using a spinless time-dependent Anderson-Newns Hamiltonian, which cannot be justified in any way. Multiple atomic orbitals are another source of degeneracy and correlations, and the neglect of such correlations can lead to qualitatively incorrect results.[10]

In this work, we present a quantum mechanical time-dependent calculation that includes the neutralization to the ground and first excited states of He in a correlated way, according to a Coulomb-blockade-like effect.[11] The model allows us to calculate the ion-survival probability, improving the agreement between theory and LEIS experiment, and to show that resonant neutralization to the He first excited state followed by Auger deexcitation can account for the complex energy dependent fine structure in the He^+/Al induced electron emission spectra. This fine structure is obtained experimentally through the application of factor analysis, as it was previously suggested.[12]

II. THEORY

In order to evaluate the effect of including the neutralization to the He excited state in addition to the ground state, on LEIS and secondary electron emission (SEE) in He^+/Al collision experiments, we perform a quantum mechanical calculation that includes both neutralization channels. To account for the ground and first excited states as possible final charge configurations, an appropriate calculation is required where only one electron transference (either to the He 1*s* or to the

He $2s$) is allowed, inhibiting the He negative charge configuration. This kind of calculation is achieved by using a developed formalism based on the infinite-correlation approach to the Anderson Hamiltonian.[11] In a simplified picture, by considering frozen the spin component of the first electron in the He^+, a second electron with the same spin component is responsible for the neutralization to the excited state $(1s\uparrow 2s\uparrow)$, while a second electron with the opposite spin component is responsible for the neutralization to the ground state $(1s\uparrow 1s\downarrow)$. The Hamiltonian including resonant and Auger processes can be written as

$$H = \sum_{k,\sigma} \varepsilon_k n_{k\sigma} + \sum_{\sigma} E_\sigma n_\sigma + \sum_{k,\sigma} [V_{k\sigma} c_{k\sigma}^\dagger b^+ c_\sigma + \text{H.c.}] + \{\text{Auger neutralization terms}\}.$$

Here, k denotes the band states of the solid (the valence and the core ones) with energy values ε_k, and $c_{k\sigma}^+$ creates an electron in a band state of the solid with spin projection σ. The operator c_σ destroys an electron either in the $1s$ ($\sigma = \downarrow$) or $2s$ ($\sigma = \uparrow$) He states; the energies, corresponding to the $1s$ and $2s$ neutralization channels, are defined as total energy differences:

$$E_\uparrow = E_{tot}(1s^1 2s^1) - E_{tot}(1s^1),$$

$$E_\downarrow = E_{tot}(1s^2) - E_{tot}(1s^1).$$

In this form, $\langle n_\sigma \rangle$ gives the He ground state configuration probability for $\sigma = \downarrow$ and the He excited state configuration probability for $\sigma = \uparrow$.

The boson operator b^+ (b) ensures the projection on the correct subspace through the constraint relation

$$b^+ b + \sum_\sigma n_\sigma = 1,$$

and the Auger terms refer only to the ground state neutralization.

The important question of whether Auger and resonant neutralization mechanisms should be treated coherently or independently has been answered for the case of considering only the ground state of He.[13] In that case, the different ion-surface distances at which both mechanisms take place allow us to treat them separately, i.e., the Auger process within a semiclassical approximation (SCA) and keeping the quantum character only for the resonant process. The same conclusion is not evident in the present case, where a resonant neutralization to a more spatially extended state is involved. In this case, a full quantum calculation including all the processes is possibly required, mainly for low kinetic energies where Auger neutralization becomes more important.

In this work, in order to explore the mechanisms responsible of the main experimental features, we treat the Auger process within the SCA and perform the quantum calculation only for the resonant processes involving the ground and excited states. The Auger deexcitation processes have transition rates that are approximately 1 order of magnitude smaller than the transition rates for resonant charge exchange.[9] Therefore, it is expected that resonant neutralization to the first excited level can be in first order treated without taking deexcitation into account.

Within this model and keeping in mind that for the lowest kinetic energies a full quantum calculation could be required, the total ion-survival probability, disregarding the reionization process, is given by

$$P^+ = (1 - \langle n_\uparrow \rangle - \langle n_\downarrow \rangle) P_{Auger}^\dagger. \quad (1)$$

In this expression, $(1-\langle n_\uparrow \rangle - \langle n_\downarrow \rangle)$ is the ion-survival probability for the case of resonant neutralization processes, while $P_{Auger}^+ = \exp[-0.036(1/v_{in} + 1/v_{out})]$ is the corresponding one for the Auger neutralization mechanism.[2] In the present calculation, $v_{in} = v_{out} = v$, where v is the ion velocity in atomic units.

Calculation of the neutralization probabilities

The average occupations are calculated from

$$\frac{d\langle n_\sigma(t)\rangle}{dt} = 2\,\text{Im} \sum_k V_{\sigma k}(t) \langle c_\sigma^\dagger b c_{k\sigma} \rangle_t,$$

where the crossed term $\langle c_\sigma^+ b c_{k\sigma} \rangle_t$ is given by the following expression

$$\langle c_\sigma^\dagger b c_{k\sigma} \rangle_t = -(1/2) \int_{t_0}^t d\tau V_{k\sigma}(\tau) \{F_{\sigma\sigma}(\tau,t) - [2f_<(\varepsilon_k) - 1] G_{\sigma\sigma}(\tau,t)\} \exp[i\varepsilon_k(\tau - t)].$$

Here, $f_<(\varepsilon_k)$ is the Fermi distribution. The required Green's functions defined in the mixed fermions-boson space,

$$G_{\sigma\sigma}(t,t') = i\Theta(t'-t) \langle \{c_\sigma^\dagger(t') b(t'), b^+(t) c_\sigma(t)\} \rangle,$$

$$F_{\sigma\sigma}(t,t') = i \langle [c_\sigma^\dagger(t') b(t'), b^+(t) c_\sigma(t)] \rangle,$$

are solved for the case of two nondegenerate states by following the procedure of Ref. 11. This model calculation is based on the equations of motion closed up to a second order in the atom-surface interaction, and it has been proven to provide confident results in a very efficient way for dynamical processes.[11]

By using a linear combination of atomic orbitals expansion of the solid band states (k), we can finally write

$$\frac{d\langle n_\sigma \rangle}{dt} = -\,\text{Im} \sum_{i,j,R_s} \int_{-\infty}^{\infty} d\varepsilon \rho_{i,j}(\varepsilon) V_{\sigma,iR_s}(t) \int_{t_0}^t d\tau V_{jR_s,\sigma}(\tau) \times \{F_{\sigma\sigma}(\tau,t) - [2f_<(\varepsilon) - 1] G_{\sigma\sigma}(\tau,t)\} \exp[i\varepsilon(\tau - t)],$$

where the indices i and j refer to the states of the surface atom centered at R_s, and $\rho_{i,j}(\varepsilon)$ is the surface local density of states (LDOS). The LDOS of the Al(100) was already presented in previous works.[2,3]

The atom-atom hopping terms $V_{j\sigma}$ are obtained from a bond-pair model of the atom-surface interaction[14] by using

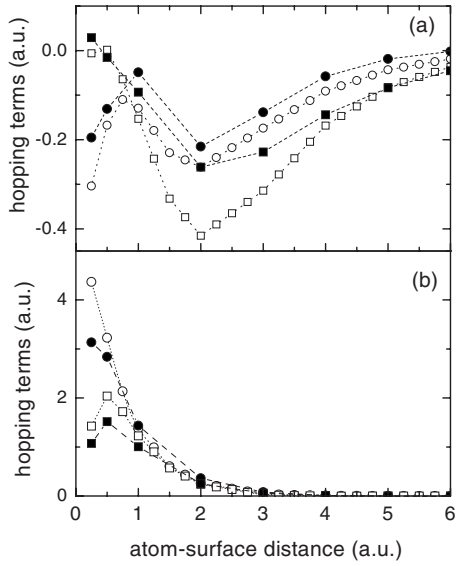

FIG. 1. Coupling terms $V_{j\downarrow}$ as a function of the atom-surface distance. Full symbols correspond to calculation using both He states, and empty ones to calculation omitting the He $2s$. Square symbols are used for the He $1s$ coupling with the Al np_z, and circles for the coupling with the Al ns. (a) Al $3s$ and Al $3p_z$ states; (b) Al $2s$ and Al $2p_z$ states.

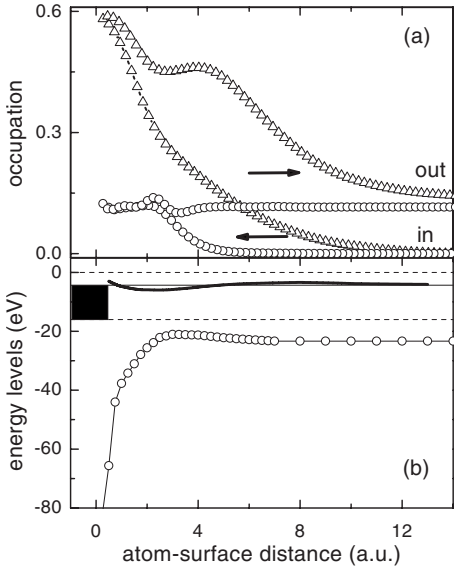

FIG. 2. (a) The evolution along the ion trajectory of the neutralization probabilities to the ground state (circles) and to the excited state (triangles), for incoming ion energy of 5 keV. By "in" we denote the incoming part, and by "out" the outgoing one. (b) The energies of the ground state $E_{\downarrow}$ (circles) and of the excited state $E_{\uparrow}$ (solid line) as a function of the atom-surface distance. The Al occupied valence band is denoted by the gray area.

Gaussian-type functions for describing the states of helium $(1s,2s)$ and of aluminum $(1s,2s,2p,3s,3p)$.[15] In Figs. 1(a) and 1(b), we compare the hopping terms $V_{j\downarrow}$ with the respective ones used in Refs. 2 and 3 that were calculated by considering only the $1s$ state on the helium site. The same dependence with the distance to the surface is observed for both cases, but a large basis set ($1s$ and $2s$) leads to smaller values of the hopping integrals.

Normal to the surface ion trajectories and the interaction with only one atom of the surface are considered, and the turning points (between 0.25 and 0.50 a.u.) are calculated from the helium-aluminum interaction energy.

III. RESULTS CONCERNING LOW ENERGY ION SCATTERING

In Fig. 2, panel (a), we show the evolution of the probabilities of the ground ($\langle n_{\downarrow}\rangle$) and excited ($\langle n_{\uparrow}\rangle$) neutral configurations along the trajectory for 5 keV incoming He^+ ions, and their corresponding energies $(E_{\downarrow},E_{\uparrow})$ as a function of the distance from the surface calculated as in Ref. 7 in panel (b). We can see the downshift below the Fermi level of the energy of the excited state, $E_{\uparrow}$, which makes an important probability of neutralization to this state possible. This channel is opened at distances larger than the ones operative for the ground state neutralization due to its more extended character, and the occupation becomes important at distances closer to the surface due to the energy resonance with the Al valence band. The excited state neutralization occurring at large ion distances from the surface limits the ground state occupation due to the Coulomb blockade effect associated with the energetically nonfavorable negative configuration.

The resonant neutralization probabilities to ground and excited states, $\langle n_{\downarrow}\rangle$ and $\langle n_{\uparrow}\rangle$, are shown in Fig. 3(a) as a function of the inverse of velocity. Also shown is the resonant neutralization probability obtained from the spinless calculation that considers the ground state as the only possible channel. We observe that $\langle n_{\downarrow}\rangle$ and $\langle n_{\uparrow}\rangle$ are comparable for large velocities, while for smaller velocity values, the neutralization to the ground state becomes more important. The results depicted in Fig. 3(b) show that the calculated total ion fraction P^+ including Auger neutralization [see Eq. (1)] follows the experimental trends as a function of the inverse of the ion velocity[2] only in the case of considering both neutralization channels. The calculation was performed in the range of large incoming kinetic energies (>1 keV), for which expression (1) is expected to be a rather good approximation. We observe a clear improvement in the theoretical ion fractions when the excited state is included. The interference between the $1s$ and $2s$ channels, originated in a Coulomb blockade effect, changes substantially the ground state neutralization when including the excited state channel. In the same way, we expect interference effects when resonant and Auger mechanisms are simultaneously taken into account.

IV. RESULTS CONCERNING ION-INDUCED ELECTRON EMISSION

A. Experimental setup

The experiments were done in a commercial surface analysis system (Perkin Elmer SAM 590A) equipped with a single cylindrical mirror analyzer (CMA), and the base pres-

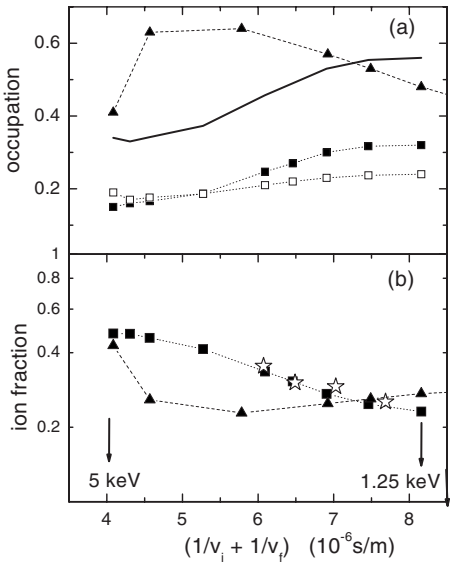

FIG. 3. (a) The resonant neutralization probability to the ground state (full squares) and to the excited state (empty squares) as a function of the inverse velocity. The total probability in this case is denoted by the full line. The resonant neutralization probability by including only the ground state corresponds to the triangle symbols. (b) The ion fraction P^+ (see text) as a function of the inverse velocity: considering ground and excited states of He (full square symbol) and by considering only neutralization to the ground state (full triangles). The empty stars correspond to the available experimental results.

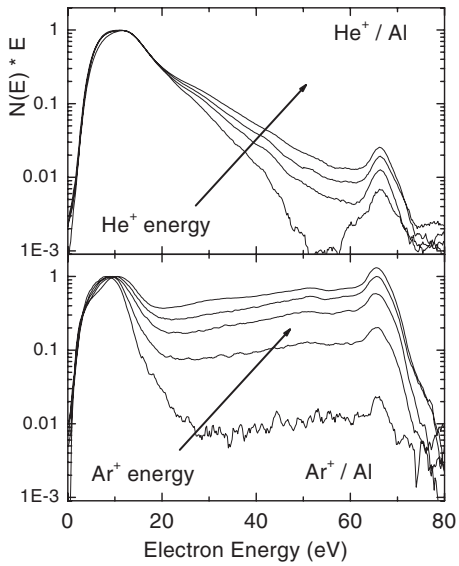

FIG. 4. Electron energy spectra induced by He^+ and Ar^+ bombardment for energies between 2 and 5 keV and between 1 and 5 keV, respectively. The curves are normalized to the true secondary peak and the spectra are not corrected by the electron analyzer transmission ($\propto E$) to enhance the high electron energy structure variations.

sure was in the low 10^{-10} Torr range. The angle of incidence of impinging ions is 58°, and the emitted electrons are averaged along the acceptance angle of the CMA. The sample is obtained by evaporation of pure (99.999) Al in UHV conditions, and its purity is controlled by means of Auger electron spectroscopy. The sample is slightly polarized (−6 V) in order to ensure the collection of low energy electrons, overcoming the difference between sample and analyzer work functions. The electrons are post accelerated, after the energy analysis (200 V), to take into account the Channeltron differential sensitivity. The results are not corrected for the analyzer transmission ($\propto E$) in order to enhance the sensitivity of high energy SEE yield.

In Fig. 4, we show the electron energy spectra for some impinging energies for He^+ and Ar^+ ions on aluminum. A large contribution from Auger neutralization (AN) of incoming ions, the main low energy peak, is expected for both types of ions. On the other hand, the high energy electrons (~68 eV) are identified as coming from the Al_{LVV} and Al_{LMM} Auger transitions.[12,16] The secondary electrons coming from the plasmon deexcitation,[17] at Ep(16 eV) − ϕ(5 eV), are not apparent in our results. The startling feature in the He/Al system is the broad shoulder appearing around 20–30 eV. This contribution is absent in the case of Ar/Al, and it cannot be attributed to a broadening of the levels with the increasing projectile energy; note, for instance, the absence of such a broadening in the low energy peak.

Most of the time, it is very difficult to deconvolute the different SEE mechanisms due to the contribution of electrons coming from the collision cascade. In order to improve the identification of such different mechanisms, we have recently introduced factor analysis (FA) as a data treatment method in this area.[12] The power of FA[18,19] is its ability to identify linearly independent component (basis) in a series of spectra taken under determined conditions. The first step in FA is the determination of the minimum number of pure components required to describe the complete series of spectra under study. The simple idea beyond FA is that the determinant of any matrix with linearly dependent columns or rows is null. The problem is reduced then to determine the number of physically meaningful nonzero eigenvalues. This work can be performed straightforwardly with the aid of several test methods.[18,19] Once the number of independent components is known, the shape of each one, and its weight along the experimental series, is determined through a least squares fit procedure.

The application of FA to the He^+/Al system gives two independent components, like we reported for Ar.[12] In Fig. 5, we summarize the FA results for He/Al on the left column and for Ar/Al on the right one. In the first row, we show the physical meaningful basis for both systems. In the second row, we show the weights of each component as the ion energy is increased. The analysis of this energy dependence gives us one interesting result. As we already pointed out, the apparent energy threshold for base 2 for Ar^+ on Al is in agreement with the energy threshold for the L shell excitation in symmetric Al-Al collision triggered by Ar^+ energy transference.[20] The energy threshold for He^+ on Al is clearly larger. The identification of possible mechanisms is rather straightforward for some cases. Following our previous assignments,[12] it is apparent that the first components are related in both cases to Auger neutralization. The different

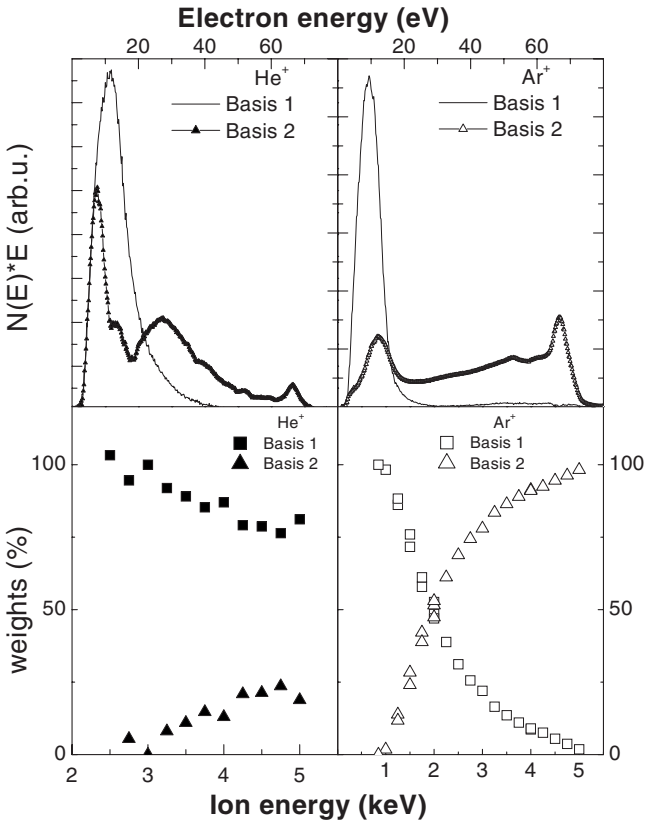

FIG. 5. Factor analysis results. First row: physical meaningful basis for He and Ar on Al. Second row: energy dependence of the weights of each component for He and Ar as a function of the ion energy.

widths of both components is related to the different available potential energies for the Auger neutralization in He^+ and Ar^+ transitions. The most interesting features are, however, associated with the second basis. In the case of Ar^+, we already identified electrons coming from the Al_{LMM} Auger (~70 eV) transition and plasmon deexcitation (~11 eV). Since FA identifies as one component those structures having the same energy dependence, we could ascribe plasmon excitation to fast Auger electrons in this case. For He^+ on Al, basis 2 has a richer structure. We can identify, using Ar basis as fingerprint when applicable, the Al_{LMM} Auger electrons, quite less important than for Ar, a low energies peak corresponding to the electron cascade, a seemingly plasmon deexcitation peak (~11 eV), and a broad peak around 20–25 eV. There are two possible mechanisms for plasmon generation: (i) energetic Al_{LVV} Auger electrons, as in the Ar^+ case,[12] and (ii) plasmon potential excitation.[17] However, we can disregard the first possibility based in the low production of energetic Auger electrons and the second one because it should belong to basis 1, in the case it was related to a potential mechanism. Looking for an explanation for the broad structure around 25 eV, we found a different possible interpretation of this "plasmonlike peak," as we show below. Finally, the peak appearing at the lowest energy in the He second component can be ascribed to the low energy cascade electrons, generated by base 2 more energetic ones. The

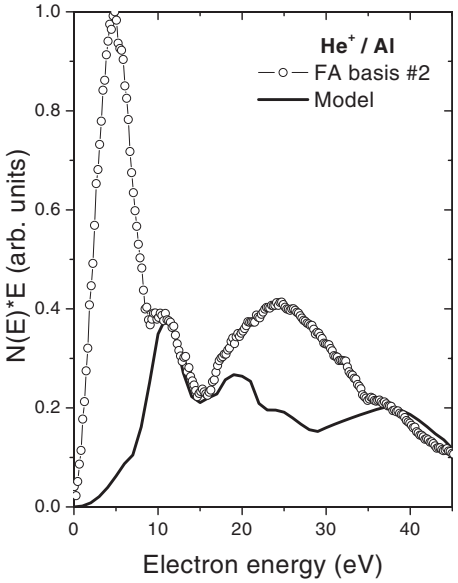

FIG. 6. Solid line: Calculated electron emission (see text). Open circles: Basis 2 for He^+ on Al.

weights of each component in the He^+/Al spectra [Fig. 5(a)] show an apparent threshold over 2 keV.

B. Model calculation of high energy electron spectrum

In order to check if the previously discussed Auger deexcitation coming from the He $1s^12s^1$ configuration may account for the high energy structure found in the He^+/Al secondary electron spectra, we calculate this spectrum within the SCA as

$$\frac{dN(E)}{dt} = [\Delta_s \rho_s(E_\uparrow - E_\downarrow + E) + \Delta_p \rho_p(E_\uparrow - E_\downarrow + E)] \times \langle n_\uparrow \rangle f_<(E_\uparrow - E_\downarrow + E),$$

where $\rho_{s(p)}(\varepsilon)$ is the local and partial density of states of the Al surface, $f_<(\varepsilon)$ is the Fermi function, $\langle n_\uparrow \rangle$ is the probability of occurrence of the excited state configuration, and $\Delta_{s(p)}$ is related with the transition matrix element. The results are obtained by assuming $\Delta_{s(p)}$ constant and limited to distances smaller than 7 a.u. Here, we can only consider the *indirect* Auger deexcitation that is the emission of one atom electron via the tunneling of one metal electron. This one is expected to be dominant for atom location not very far from the surface.[21]

The Auger spectra obtained in this way are corrected by the energy analyzer transmission to compare with the experimental results. In Fig. 6, we compare the theoretical calculation with basis 2 obtained through FA of He^+/Al experiments. We can identify, at least in a rough way, the experimentally observed peaks as coming from the Auger deexcitation following the resonant neutralization to the first He excited state. The low energy peak (~12 eV) corresponds to transitions occurring at distances around 3 a.u., where an important occupation of the excited state is regis-

tered in the outgoing trajectory, and the energy difference between both levels is lower than the asymptotic value (Fig. 2). The larger energy peak corresponds to deexcitations occurring in closer collisions where the level downshift is more pronounced. The weights of these peaks will depend on the distance dependence of $\Delta_{s(p)}$. A more rigorous calculation, where trajectory and velocity effects in the level shifts and widths are included, could justify the appearance of more energetic electrons (around 25 eV). In the same way, smaller angle trajectories would involve longer times close to the surface increasing the relative weight of electron emission at larger energies. On the other hand, for lower ion incoming energies, the increasing probability of Auger neutralization to the ground state and the promotion of the He 1*s*, which favors the resonant mechanism to this level, will tend to suppress the emission of high energy electrons in agreement with the experimental results.

V. CONCLUSIONS

Through an adequate quantum mechanical time-dependent calculation of resonant neutralization to the ground and first excited states, we can provide an answer to the discrepancies between theory and experiment in He^+/Al experiments on low energy ion scattering spectroscopy and ascribe the observed fine structure in electron emission to Auger deexcitation occurring at different ion-surface distances.

ACKNOWLEDGMENTS

This work was financially supported by ANPCyT through PICT14730 and 14724, CONICET through PIP 5277, and UNL through CAI+D grants. Helpful discussions with F. Flores, R. Monreal, R. Baragiola, R. Vidal, and S. Montoro are fully acknowledged.

[1] H. D. Hagstrum, Phys. Rev. **96**, 336 (1954).
[2] E. C. Goldberg, R. C. Monreal, F. Flores, H. H. Brongersma, and P. Bauer, Surf. Sci. Lett. **440**, L875 (1999).
[3] N. P. Wang, E. A. García, R. Monreal, F. Flores, E. C. Goldberg, H. H. Brongersma, and P. Bauer, Phys. Rev. A **64**, 012901 (2001).
[4] R. Cortenraad, A. W. Denier van der Gon, H. H. Brongersma, S. N. Ermolov, and V. G. Glebovsky, Phys. Rev. B **65**, 195414 (2002).
[5] J. C. Lancaster, F. J. Kontur, G. K. Walters, and F. B. Dunning, Phys. Rev. B **67**, 115413 (2003).
[6] S. Wethekam and H. Winter, Surf. Sci. **596**, L319 (2005).
[7] W. More, J. Merino, R. Monreal, P. Pou, and F. Flores, Phys. Rev. B **58**, 7385 (1998).
[8] G. E. Makhmetov, A. G. Borisov, D. Teillet-Billy, and J. P. Gauyacq, Europhys. Lett. **27**, 247 (1994).
[9] R. J. A. van den Oetelaar and C. F. J. Flipse, Phys. Rev. B **52**, 10807 (1995).
[10] D. C. Langreth and P. Nordlander, Phys. Rev. B **43**, 2541 (1991); J. B. Marston, D. R. Andersson, E. R. Behringer, B. H. Cooper, C. A. DiRubio, G. A. Kimmel, and C. Richardson, *ibid.* **48**, 7809 (1993).
[11] E. C. Goldberg, F. Flores, and R. C. Monreal, Phys. Rev. B **71**, 035112 (2005).
[12] N. Bajales, S. Montoro, E. C. Goldberg, R. A. Baragiola, and J. Ferrón, Surf. Sci. Lett. **579**, L97 (2005).
[13] E. A. García, N. P. Wang, R. C. Monreal, and E. C. Goldberg, Phys. Rev. B **67**, 205426 (2003).
[14] P. G. Bolcatto, E. C. Goldberg, and M. C. G. Passeggi, Phys. Rev. A **50**, 4643 (1994).
[15] S. Huzinaga, J. Chem. Phys. **42**, 1293 (1964).
[16] R. A. Baragiola, E. V. Alonso, and H. J. L. Raiti, Phys. Rev. A **25**, 1969 (1982).
[17] R. A. Baragiola and C. A. Dukes, Phys. Rev. Lett. **76**, 2547 (1996).
[18] E. R. Malinowski, *Factor Analysis in Chemistry*, 2nd ed. (Wiley, New York, 1991).
[19] V. Atzrodt and H. Lange, Phys. Status Solidi A **79**, 489 (1983); **82**, 373 (1984); R. Vidal and J. Ferrón, Appl. Surf. Sci. **31**, 263 (1988); L. Steren, R. Vidal, and J. Ferrón, *ibid.* **29**, 418 (1987); J. Steffen and S. Hofmann, Surf. Sci. **202**, L607 (1988).
[20] R. A. Baragiola, E. V. Alonso, and H. J. L. Raiti, Phys. Rev. A **25**, 1969 (1982).
[21] M. A. Cazalilla, N. Lorente, R. D. Muino, J. P. Gauyacq, D. Teillet-Billy, and P. M. Echenique, Phys. Rev. B **58**, 13991 (1998).